A new type of truss joint for prevention of progressive collapse

Citation for published version:
Yan, S, Zhao, X, Chen, Y, Xu, Z & Lu, Y 2018, 'A new type of truss joint for prevention of progressive collapse' Engineering Structures, vol. 167, pp. 203-213. DOI: 10.1016/j.engstruct.2018.04.031

Digital Object Identifier (DOI):
10.1016/j.engstruct.2018.04.031

Published In:
Engineering Structures

A new type of truss joint for prevention of progressive collapse

Shen Yan [b,1], Xianzhong Zhao [a,b], Yiyi Chen [a,b], Zhenyu Xu [b], Yong Lu [c]

a. State Key Laboratory of Disaster Reduction in Civil Engineering, Tongji University, Shanghai 200092, China;

b. College of Civil Engineering, Tongji University, Shanghai 200092, China;

c. Institute for Infrastructure and Environment, School of Engineering, University of Edinburgh, Edinburgh EH9 3JL, U.K;

1. College of Aerospace Engineering and Applied Mechanics, Tongji University, Shanghai 200092, China.

Abstract: This paper presents a study on a new type of truss joint (Pinned-Slidable or PS joint) that is designed to maximize the function of catenary action upon a sudden member removal. The basic idea for a PS joint is such that it is fixed on the bottom chord without sliding under the design load, but can slide along the bottom chord to help distribute the unbalanced tensile forces that the catenary action generates on different bottom chord members. The sliding resistance of this joint is provided by the friction generated by the preloaded bolts and the shear resistance of a locking rod, which can be designed according to the proposed design schemes. A Warren truss with PS joints as the bottom joints (Truss-PSJ) has been designed and tested under a scenario of a sudden removal of one of its diagonal members, and the response of the structure is compared with that of an identical truss model except for its non-slidable joints (truss-PJ). Results show that significant catenary action develops in the bottom chord of the remaining structure in the process of establishing a new equilibrium state after the member removal, and the catenary action tends to generate much larger tensile forces in the bottom chord members in the mid-span than in the neighboring bottom chord members, leading to the sliding of a PS joint. By comparing the test results of truss-PSJ with those of its counterpart truss-PJ, the benefits of the PS joints have been clearly demonstrated. The sliding of the PS joint not only releases the excessive unbalanced forces between neighboring members and thus enables a fuller development of the catenary action, but also facilitates the adaptation of the remaining structure towards a new balanced state with a near-optimal deformation shape. A finite element analysis has also been conducted to confirm the above experimental observations, and to demonstrate the performance of PS joints under other progressive collapse scenarios. Furthermore, a method for determining the sliding resistance of PS joints is also proposed.

Keywords: slidable truss joints; progressive collapse; catenary action; adaptive system;

1. Introduction

Truss structures are widely used in roofing systems and bridges. Even built with many redundant members, a truss may still collapse due to the spread of the initial failure of one or a few load-bearing members. This was what happened to the space truss roof of the Hartford Civic Center, which collapsed in 1978 after a few compressive members buckled [1]. Another example of accident involved the collapse of the Minneapolis I-W35 steel truss bridge in 2007; the primary cause of the collapse was deemed to be the fracture of a few undersized gusset plates [2]. Recent years have therefore seen increasing attention to the progressive collapse of truss structures in the research and practicing communities.

A number of studies have been conducted to investigate the key factors affecting the collapse resistance of truss roofs and truss bridges. These factors include the location of initial failure [3-5], the stiffness of the joints [6], the live load intensity [7] and the live load distribution and span ratio of continuous truss bridges [8]. The collapse-resisting mechanisms of truss structures have been found to vary depending upon the location of the initial failure. For planar trusses, catenary action provides the bridge-over capacity for the remaining structure when the initial failure occurs at a top chord or a diagonal member, while arch action plays a dominant role in the collapse resistance under a bottom chord loss scenario [5, 6]. For a truss roof system, the tie forces provided by the roof braces help transfer the external load on the damaged truss to the neighboring undamaged truss [7]. With regard to the analysis methods, USR [9], Goto et al. [10] and Khuyen and Iwasaki [11] investigated the dynamic amplification factor to be used in association with a linear static analysis for steel truss bridges. Yan et al. [5] presented an improved FE approach, by applying viscous damping forces and controlling the stiffness degradation of the removed member, to improve the efficiency of nonlinear dynamic analysis of truss structures. On the experimental front, Zhao et al. [6] provided a comprehensive solution for the testing of progressive collapse resistance of truss structures allowing for an abrupt initiation of a local failure and development of the dynamic responses.

Generally speaking, to prevent the collapse of a structure in a progressive manner, one may always look into identifying the critical members whose initial failure could cause the most severe disruption and damage of the structural system, and enhance these members so that they do not fail when the structure encounters plausible exceptional loads. According to [5], for a planar truss these members include all members at the mid-span and the end-span bottom chord member. However, there are events which are unpredictable, for example accidental explosions and accelerated fatigue due to construction errors, and for such situations it would be impractical or impossible to completely prevent initial local failures. In this respect, a more viable approach to mitigating the collapse risk of truss structures would be to ensure a desirable load-carrying capacity through adequate collapse-resisting mechanisms in the event of a local failure.

During the process of regaining a balanced state through the collapse-resisting mechanisms, there would be certain structural members that are at a higher risk of subsequent failure than other members. It is shown in [6] that for a truss structure subjected to the loss of a diagonal member or a bottom chord member, highly non-uniform tension could be generated in different bottom chord members during the development of the catenary action. Fig. 1 presents a brief illustration of the test results of a Warren truss with pinned connection between diagonal members and continuous chords (truss-PJ) following a sudden removal of a diagonal member. It was found that in this case the central bottom chord member (BC3) experienced a considerably larger tensile force than other chord members. Such members are normally regarded as the "key elements" which can be exposed to much higher risk of follow-on failure and consequently lead to the collapse of the entire structure.

Clearly, mitigating the risk of failure of the key elements is crucial to increasing the overall collapse resistance of the structure. An ideal situation would be that all structural members are rendered the same risk of subsequent failure. One of the possible solutions is to enhance these key elements by increasing their cross sections. However, more often the key elements depend on the location of the initial failure and thus cannot be predicted in advance.

Moreover, it is not an efficient approach for the key elements to be designed "passively" with a much larger strength to counter the extra loads which would only occur in an accidental condition. Instead, finding an effective way to "proactively" improve the re-distribution of the loads to other members would be a more desirable strategy. Based on the above considerations, this paper presents a new type of truss joint with an aim to release the unbalanced forces among bottom chord members, and thus enable a "proactive" resistance enhancement against progressive collapse.

The following sections describe the assembly of the new type of joints and its working mechanism under a progressive collapse scenario. A planar Warren truss was built with the new joints and it was tested under a sudden removal of a diagonal member. The experimental programme is described and the test results are compared with the results obtained previously from a comparable truss but without the new type of joints to demonstrate the advantages of the new joints in improving the collapse resistance of the structure. A method for determining the usage of the new joints in a truss and their design sliding resistances is then put forward. Finite element (FE) investigations are also conducted to confirm the experimental observations, and to demonstrate the performance of this new type of joints under other progressive collapse scenarios.

2. Concept of the new joint and its working mechanism

The concept of the new joint involves the following attributes: (a) under design loads, the joint behaves the same as a commonly used joint such as a welded joint, (b) when catenary action is being developed in the bottom chord under a progressive collapse scenario, the mechanism of the joint is activated so that it helps to realize a uniform tension in the bottom chord members, (c) to enhance the catenary action function, the joint also realizes a pinned connection between a diagonal member and the bottom chord, and this helps prevent early buckling of the diagonal members, which would otherwise experience significant distortions as the catenary action develops [6].

2.1. Prototype design

According to the above objectives for the new truss joint, the prototype of the joint is designed. Fig. 2 illustrates the components of the joint and the assembly method. Firstly, two steel blocks are fixed onto the bottom chord through four preloaded bolts. The upper steel block has a lug plate on its top surface and a half-cylinder groove on its bottom surface, and the lower steel block has an identical half-cylinder groove on its top surface. The position of the paired steel blocks on the bottom chord is guaranteed by a locking rod, which threads through the vertical holes at the center of the steel blocks and the holes in the bottom chord at the joint location. The diagonal members, which are fitted (through weld) with a connection coupler at their bottom end, are jointed to the bottom chord by connecting the ear plates of the coupler to the lug plate of the upper steel block through pins.

Under design loads, the friction generated by the preloaded bolts and the shear resistance provided by the locking rod are combined in a certain way, which is to be discussed later, to provide the sliding resistance required for the steel blocks to stay immobilized on the bottom chord. When catenary action is developed under a progressive collapse scenario, if the tensile force difference between the bottom chord members on two sides of a PS joint (referred as the unbalanced force of this joint) exceeds the sliding resistance, the locking rod shall break and the steel blocks can slide along the bottom chord. This will largely release the unbalanced force. Therefore, the objectives of (a) and (b) are met. As a matter of fact, the “ear plate - pin - lug plate” design for the connection of diagonal members to the bottom chord already guarantees a pin-connected condition for the diagonal members to the bottom chord, in this way the objective (c) is also satisfied.

Hence, this new joint is named as Pinned-Slidable Joint (abbreviated as PSJ or PS joint). It is noted that the PS joint is similar to the pinned joint connector in the previous test truss-PJ, except that in the pinned joint connector the steel blocks are permanently fixed onto the bottom chord through welding in addition to the preloaded bolts and locking rod, allowing no relative sliding at any stage of the response.

2.2. Control of sliding resistance

The sliding resistance is controlled through the number of the preloaded bolts and size of the locking rod. Fig. 3 illustrates schematically the sliding resistance versus sliding displacement curves. The curves are based on two simple yet important physical phenomena, namely, a) the locking rod lags behind the preloaded bolts in providing sliding resistance due to its installation tolerance, and b) the maximum static friction generated by the preloaded bolts (F_S) is generally larger than the kinetic friction generated by the same bolts (F_K).

For a PS joint being immobilized on the bottom chord, the sliding resistance is solely provided by the static friction. If the maximum static friction F_S is overcome by the unbalanced force of this joint, the joint starts to slide along the bottom chord, and the sliding resistance shall experience an instantaneous drop until the locking rod starts to play its role. Depending on the shear resistance of the locking rod, the PS joint can have two different modes of subsequent performance, i.e., mode 1 and mode 2 in Fig. 3. Accordingly, these two modes correspond to two design schemes.

If the design sliding resistance of a PS joint (R) can be fully achieved by the static friction generated by the preloaded bolts, the PS joint should follow mode 1, thus the locking rod must be small or can even be cancelled. This design scheme can be referred to as "strong bolts, weak rod". In this respect, the shear resistance of the locking rod (S_L) should be no larger than the friction change during transition from static friction to kinetic friction:

$$\begin{cases} F_S = R \\ S_L = S_1 \le F_S - F_K \end{cases} \tag{1}$$

The preloaded bolts and the locking rod can thus be designed. By assuming a circumferentially uniform pressure between the inner surface of the steel blocks and the bottom chord member, the product of the number of the bolts (n) and the preload in each bolt (P) is

$$n \cdot P = \frac{R}{\pi \mu_S} \tag{2}$$

where μ_S is the static friction coefficient. The shear resistance of the locking rod should satisfy

$$S_L \leq \left(1 - \frac{\mu_K}{\mu_S}\right) \cdot R \tag{3}$$

where μ_K is the kinetic friction coefficient.

Sometimes the number or the size of the preloaded bolts might be insufficient due to architectural and constructional considerations, thus a strong locking rod must be used to fill the gap between the design sliding resistance and the kinetic friction generated by the preloaded bolts. In this case, the design scheme can be referred to as "weak bolts, strong rod", and the PS joint follows mode 2:

$$\begin{cases} F_S < R \\ S_L = S_2 = R - F_K \end{cases} \tag{4}$$

The shear resistance of the locking rod can thus be designed as

$$S_L = R - \pi \mu_K \cdot n \cdot P \tag{5}$$

The determination of the shear resistance for the PS joints will be discussed later in Section 5.

3. Experimental study of truss with PS joints

To verify the effectiveness of incorporating the new joints in a truss structure, an experimental study was first carried out. The details of the experimental programme and the main test results are presented in this section.

3.1. Test model design

The tested truss model with the use of the PS joints along the bottom chord is referred as truss-PSJ. To facilitate a direct comparison between truss-PSJ with truss-PJ mentioned earlier, the geometric and material properties of truss-PSJ was kept the same as that of truss-PJ.

Truss-PSJ had a span of 4.0 m and a height of 0.45 m, as shown in Fig. 4. The top chord (TC) and the bottom chord (BC) were continuous, and the diagonal members (DM) were connected to the top chord and the bottom chord through pinned joint connectors and the new PS joints, respectively. All members were constructed using DIN2391 St.35 steel pipes, and the cross-sections and mechanical properties are shown in Table 1. The two edge supports (SJ1 and SJ2) were made as fixed pins with full horizontal restraints. The design loads were applied as point loads at the top joints: 1.0 kN was applied on each edge top joint (TJ1 and TJ5) and 2.0 kN was applied on each middle top joint (TJ2, TJ3 and TJ4).

The sliding resistances of PS joints must be carefully designed. Otherwise, a PS joint with sliding resistance smaller than the required immobilizing force under design loads shall experience unwanted sliding prior to member removal, and a PS joint with excessively large sliding resistance tends to always stay immobilized on the bottom chord even under a severe progressive collapse scenario. For a demonstrative purpose, the sliding resistance of each PS joint has been determined based on the testing results of truss-PJ with non-slidable joints. Fig. 5 shows the unbalanced force of each bottom joints in truss-PJ. It is observed that the unbalanced force of BJ2 increased dramatically upon the removal of DM2, while that of the other bottom joints decreased. Therefore, a sliding resistance of R = 7.5 kN was designed for BJ1 and BJ4 to guarantee their immobilized state under design loads and possible perturbations during the static loading process. For PS joint at BJ2, the sliding resistance was designed as 5.0 kN which was slightly smaller than the peak value of the unbalanced force but was much larger than the required immobilizing force (about 1.7 kN). For PS joint at BJ3, a sliding resistance of 2.0 kN would have been sufficient; however, its sliding resistance was designed to be the same as that of BJ2 (i.e., 5.0 kN) to facilitate test result comparisons between BJ2 and BJ3.

The “strong bolts, weak rod” design scheme was adopted for truss-PSJ. For PS joints at BJ1 and BJ4, the preload of each bolt and the shear resistance of the locking rod were designed according to Eq. (2) and (3):

$$P_1 = P_4 = \frac{7.5\text{kN}}{4 \times \pi \times 0.30} = 1.99\text{kN} \tag{6}$$

$$S_{\text{L}} \leq \left(1 - \frac{0.15}{0.30}\right) \times 7.5\text{kN} = 3.75\text{N} \tag{7}$$

where μ_S was taken as 0.30 for clean steel surfaces [12], and μ_K was taken as half of μ_S for clean steel-on-steel friction [13].

Bolts with nominal diameter of 6mm were used. For each bolt, the torque necessary to generate bolt preload of 1.99 kN must be estimated. The wrench torque (T) can be determined by using a general relation [13]:

$$T = K \cdot P \cdot d \tag{8}$$

where K is a constant that depends on the bolt material and size, and a value of K=0.2 may be used in this equation for mild-steel bolts; d is the nominal bolt diameter. Thus according to Eq. (8), the wrench torque was calculated to be 2.39 kN·mm, which was applied using a wrench and a forcemeter attached at its end.

Fine-machined small rods with diameter of 2.5 mm were used as the locking rods. The rod material had a tensile strength of about 320 MPa which was determined by trial, thus the shear strength was estimated to be about 256 MPa (=0.8×320MPa). Therefore, the shear resistance of a locking rod was 1.26 kN, and Eq. (7) was satisfied.

For PS joints at BJ2 and BJ3, the preload of each bolt and the maximum shear resistance of the locking rod were calculated following the above procedure. Results showed that P_2= P_3=1.33 kN, and the corresponding wrench torque is 1.59 kN·mm. The maximum shear resistance is 2.5 kN, thus the 2.5 mm-diameter rods can also be used in these two PS joints.

3.2. Test setup

Fig. 6 shows an overall view of the test setup. The test setup, including support conditions, method of applying static loads, measurement locations, as well as the location of the suddenly removed member, were also maintained the same with that of its counterpart truss-PJ. A detailed description of the general testing program can be found in [6]. A brief overview is given in what follows.

The test truss was supported at both ends with fixed pins on two reaction frames fixed onto a strong floor. Meanwhile, a pair of transparent plexiglass plates was placed on both sides of the tested truss to ensure that the tested planar truss only deformed vertically.

When the test was carried out, the test structure was first loaded to simulate a normal loading condition. The point load on each top joint was applied by means of weights (iron plates) through hanger rods that were attached to the top joint connector. The main test then proceeded with a sudden removal of a diagonal member, in this case DM2, using a member-breaking device. The member-breaking device was invented to break a predefined structural member instantaneously, and it has been used successfully in the progressive collapse tests of truss and steel dome model structures [6, 14]. The member removal time is about 0.06s.

As is generally known, a sudden removal of a member from a structure triggers a transient dynamic response with abrupt changes of the geometrical shape and internal forces. To capture the dynamic responses, a videogrammetric technique was employed with the aid of two high-speed CMOS cameras (Basler ACA 2040-180KM) to capture the full field measurement of the structural dynamic deformation in the 3D domain. The image rate was set at 180 frames per second. A dynamic strain data acquisition system (DH3820) was employed to collect the dynamic strain responses in all members at a sampling frequency of 100 Hz.

3.3 Test results and performance comparisons

Before the diagonal member DM2 was removed, all PS joints in the test truss-PSJ kept staying at their original locations on the bottom chord under the statically applied point loads. Upon the removal of DM2, the truss underwent immediate deformation and the catenary action began developing in the bottom chord. Joint BJ2 started to slide leftwards along the bottom chord at about 0.24 s after the trigger of removal of DM2. The overall shape and the truss grids underwent significant distortion. At about 0.5 s, the truss regained a balanced state with the joint BJ2 having slid for up to 143 mm, as shown in Fig. 7a. Under the re-balanced state, the overall deformation was approximately symmetric with the largest vertical displacement occurring at the mid-span of the top chord. Due to the sliding of BJ2, the balanced configuration of the current truss-PSJ clearly deviated from that of its counterpart truss-PJ in which sliding of the bottom joints was not allowed as shown in Fig. 7b.

The removal of DM2 will tend to greatly amplify the unbalanced force between bottom chord BC3 and BC2, as already demonstrated in the test of truss-PJ. Fig. 8a shows the unbalanced forces of BJ2 in both truss-PSJ and truss-PJ. In truss-PSJ, at about 0.24 s the unbalanced force rose up to about 5.29 kN, which went slightly beyond the design sliding resistance (5.0 kN) and thus triggered the sliding mechanism to come into play. With the sliding of BJ2, the unbalanced force was largely released. Fig. 8b shows the unbalanced forces of the other three bottom joints, namely, BJ1, BJ3 and BJ4. Their unbalanced forces stayed below the design sliding resistance with a large margin for the entire deformation history; as a result, these PS joints did not move.

As the sliding of BJ2 released the unbalanced tensile forces between BC2 and BC3, all bottom chord members in truss-PSJ had almost the same tensile forces in them, as shown in Fig. 9a. This is apparently different from the pattern of catenary action in truss-PJ, in which disproportionate tensile strains were found in different bottom chord members as shown in Fig. 1b. By comparing Fig. 9a to Fig. 1b, it is observed that while the tensile strain in BC3 of truss-PSJ was very much smaller than that of truss-PJ, tensile strains in other bottom chord members of truss-PSJ were a little larger than that of truss-PJ. Therefore, the sliding of joint BJ2 improved the performance of the catenary action in truss-PSJ directly, as no significant concentration of tensile force within a single member as did in truss-PJ occurred. In all, the PS joints enabled a more robust development of the catenary action in the bottom chord.

During the sliding of joint BJ2 towards its final position on the bottom chord, the load-bearing mechanism of the remaining structure went through a notable change. The pattern of alternate tensile-and-compressive internal forces in the diagonal members disappeared, and all diagonal members were under compression to transfer the point loads applied on the top joints to the supports through the bottom chord where the catenary action developed, as shown in Fig. 9b. This is different from truss-PJ, in which the undamaged truss grids on the right hand side of DM2 still behaved as typical trusses. The top chord members, on the other hand, had the compressive forces in them unloaded, with TC2, TC3 and TC4 even under certain amount of tension, as shown in Fig. 9c. Therefore, upon the removal of DM2, the remaining structure of truss-PSJ behaved more like a cable-strut structure than a typical truss, which was the result of sliding of joint BJ2. It would be wrong to assert that the load-bearing mechanism of cable-strut structures is definitely better than that of trusses, but according to the experimental data the internal forces in truss-PSJ are smaller than those of truss-PJ for almost all members. In fact, the PS joints helped truss-PSJ become an adaptive system to a certain extent, and facilitated the adaptation of the remaining structure towards a new balanced state with a near-optimal deformation shape. Adaptive ability provided by the sliding of structural components can be found in other types of civil structures as well. For example, in the flexible barriers commonly used for rockfall mitigation, the netting attached to cable ropes spanning across steel posts can slide along the cable ropes after hit by debris flows [15].

It is also noted that although the grids of truss-PSJ experienced dramatic change (for instance, the angle between DM5 and BC3 changed from 48° to 33°), no buckling was observed in any diagonal member. As a comparison, a truss with rigid connections between the diagonal members and the chord members tested in [6] collapsed due to successive buckling of several diagonal members due to grid distortions. This comparison further demonstrates the importance of adopting pinned connections between diagonal members and chord members.

4. Numerical simulation: FE model development and validation

4.1. FE modelling considerations

Finite-element investigation is carried out to assist in the interpretation of test results, as well as to investigate the performance of PS joints under the loss of a member other than the diagonal member considered in the test.

A finite-element model of truss-PSJ is developed in commercial FE package *Abaqus*, and the analyses are performed using the explicit time integration solve *Abaqus/Explicit*. The improved FE analysis procedure for progressive collapse analysis put forward in [5] is adopted. The static initial condition of the intact truss-PSJ is obtained first, and then the elements of DM2 are removed in 0.06 s corresponding to the actual time period of the member removal as observed from the physical experiment. Fig. 10 shows the overview of the FE model along with the modelling details at top and bottom joints.

The top chord members and diagonal members are modeled with two-node linear space beam elements (element type “B31”) with a pipe cross-section, and each member is modeled by 10 beam elements, which is enough to capture the potential buckling behavior under compression [5]. The bottom chord members are modeled with four-node reduced integration doubly curved shells (element type “S4R”) for simulation of PS joints’ sliding along the bottom chord. The materials of the chord members are modeled using a piecewise-linear plasticity model with stress-strain curves based on the coupon test data.

At each top joint, the joint connector is modeled with B31 elements with a rectangular cross-section and B31 elements with a circular cross-section, where elastic material model is adopted. All degrees of freedom are constrained between the joint connector and the top chord members, while the in-plane rotational degree of freedom is released between the joint connector and the diagonal members.

At each bottom joint, the top and bottom steel blocks of the PS joints (refer to the PS joint details in Fig. 2) are modeled with discrete rigid bodies, and they are assembled together through “Tie” constraint at the contact surface. Contact between the half-cylinder grooves of the steel blocks and the outer surface of the bottom chord is defined in order to simulate the sliding of the PS joints along the bottom chord. A “hard” contact with zero-penetration between contact surfaces is specified for the normal behavior. For the tangential behavior, a friction coefficient of 0.30 is specified, which is adopted as the static friction coefficient in this FE analysis. Because the cylindrical contact surfaces fit closely together, local stress concentration would not occur, and therefore the mesh size has little effect on the stress and strain calculation within the connection. Nevertheless, sufficiently small mesh size should still be adopted for the shell elements to avoid penetration between the contact surfaces. The cross-section of the bottom chord is partitioned into 16 shell elements, resulting in a uniform mesh size of about 3.7 mm. By adopting this mesh size, good convergence had already been achieved, and no penetration was observed between the contact surfaces.

Normally, the pretension of bolts in a structure can be simulated with assembly loads in *Abaqus*. However, this technique can only be employed in association with the implicit solver *Abaqus/Standard*. Since the role of the pretension bolts in the FE model is solely related to the friction, the same effect can be realized by directly simulating the static friction without explicit inclusion of the pretension bolts. In the current model, this is achieved by using a fictitious "shear stud", connecting the top steel block and the cross-section center of the bottom chord member, with a specified shear fracture limit equal to the friction resistance as would be provided by the preloaded bolts. It should be pointed out that this fictitious "shear stud" is not part of the "locking rod" and its property is specified just to represent the friction effect. The shear stud has a length of 10 mm and a rectangular cross section of 3 mm×3 mm, and is modeled with eight-node linear reduced integration brick solid elements (element type "C3D8R"). Shear stress distribution is uniform over any rectangular cross-sections of the stubby shear stud, and therefore mesh size has little influence on the calculation of shear stress. In this study, a mesh size of about 3 mm equal to the width of the shear stud is adopted. The material of the shear stud is modeled using elastic material, where a large elastic modulus of 2×10^6 MPa is assigned to reduce the bending deformation of this shear stud. For PS joints at BJ1 and BJ4, the design sliding resistance generated by the preloaded bolts is 7.5 kN, thus a shear failure limit of 833 MPa (=7500 N/9 mm^2) enables an adequate simulation for the immobilizing effect of the static friction generated by the preloaded bolts. For PS joints at BJ2 and BJ3, the shear failure limit is 555 MPa (=5000 N/9 mm^2). It is noted that as the preloads of the bolts are not modeled, the tangential friction coefficient mainly works in association with the contact pressure generated by the vertical component of the resultant force of the connecting diagonal members.

As the design of the sliding resistance follows the "strong bolts, weak rod" scheme (refer to mode 1 in Fig. 3), the shear resistance of the locking rod can be ignored without causing much difference, thus the locking rod is not included in this FE model.

The point loads are modeled with lumped masses. The out-of-plane translational and rotational degrees of freedom are fully restrained at all joints to simulate the out-of-plane constraint in the actual experiment.

4.2. Model validation and comparative results

After DM2 is removed, the FE model of truss-PSJ deformed downwards rapidly, and catenary action develops along the bottom chord with the increase of the displacements. The sliding mechanism of the PS joint at BJ2 is activated at about 0.21 s, and the final sliding distance is about 155 mm. Fig. 11 presents the comparisons between the FE predictions and the experimental measurements of the structural responses, including the balanced configuration, the vertical displacement at the mid-length of the top chord and the unbalanced force of bottom joint BJ2. Overall, good agreement is observed between the FE and the experimental results. The results demonstrate that the FE model represents well the sliding behavior of the PS joints, the dynamic responses of the remaining structure and the collapse-resisting mechanism of the tested truss, and therefore it can be applied in the extended numerical studies of other member removal scenarios.

When the removal of a different structural member is considered, it can be expected that a different sliding resistance demand for a particular PS joint will arise, so the joint sliding resistances adopted in the test programme may not apply to other member removal scenarios. Therefore, a method for determining the design sliding resistance for the PS joints to be used under all progressive collapse scenarios is required and this is discussed in the following section.

5. Sliding resistance design of the PS joints

The PS joints in a truss should function properly under different member loss scenarios. To this end, the proposed method is based on the following considerations: 1) no sliding should occur in the intact truss under design loads, and thus the sliding resistance of each PS joint should be larger than the unbalanced force of this joint under design loads; 2) but to avoid setting the sliding resistance unnecessarily too high, there is a need to identify the unbalanced forces that would occur under a variety of catenary action scenarios; 3) PS joints may not be needed for all bottom joints because for certain bottom joints the maximum unbalanced force under all catenary action scenarios can be smaller than the unbalanced force under design loads; 4) it is also important the PS joints keep immobilized on the bottom chord under bottom chord member removal scenarios to enable proper function of the arch action, and the design sliding resistance of each PS joint should also be larger than the maximum unbalanced force that would occur under arch action. Therefore, the procedure includes five steps, as illustrated in Fig. 12. The unbalanced forces of PS joints can be calculated by assuming all PS joints are non-slidable, therefore, only the most simplified FE models with all members modelled with beam elements are needed.

Step 1 calculates the unbalanced force under design loads for each bottom joint BJm (F_m^0). Linear static analysis is performed on the intact truss, thereby the axial force of each bottom chord member BCm (T_m^0) can be obtained. Then F_m^0 can be calculated by the difference in the internal forces of the two adjacent chord members:

$$F_m^0 = \left| T_m^0 - T_{m+1}^0 \right| \tag{9}$$

Step 2 calculates the unbalanced force under different catenary action scenarios for each bottom joint. Alternate Path (AP) analysis is performed on the truss by removing the top chord members one at a time. There are m bottom joints, thus in terms of re-balanced deformation shape there can be as many as m catenary action scenarios, in each of which a different bottom joint is at the lowest point of the entire bottom chord. These catenary action scenarios can be created by removing the top chord member right above this joint one at a time [5], therefore, there is no need for AP analysis of removing the diagonal members although the initial failure of a diagonal member also leads to catenary action in the bottom chord. For instance as shown in Fig. 13, the removal of diagonal members DM1 and DM2 lead to identical re-balanced deformation shapes compared with that caused by the removal of the top chord member TC1. For bottom chord joint BJm, the unbalanced force under the removal of a top chord member TCn (F_m^{TCn}) can be obtained through

$$F_m^{TCn} = \left| T_m^{TCn} - T_{m+1}^{TCn} \right| \tag{10}$$

AP analysis can be performed with varying complexities, and generally there are three analysis procedures [16]. Since the main purpose of the analysis is for sliding resistance design, a nonlinear static analysis is recommended and this is employed herein. Currently, there is no codified recommendation on the dynamic increase factor (DIF) value to be used in nonlinear static analysis of truss structures. It is shown that for a linear static analysis of steel truss bridges, the DIF varied between bridges and with the location of the removed members, but in all cases the DIF values were smaller than 1.4 [11]. For simplicity, in this study the DIF is taken as a constant value of 1.4.

Step 3 determines the usage of PS joints, namely, where PS joints are to be used. This is achieved by comparing the maximum unbalanced force under catenary action F_m^{TC} (the maximum F_m^{TCn}) against the unbalanced force under design loads F_m^0 for each bottom joint. For bottom joint BJm, a circumstance of F_m^{TC} being smaller than F_m^0 indicates that the sliding mechanism of a PS joint (if used at BJm) shall never be activated as long as the PS joint is designed to be immobilized on the bottom chord under design loads. Therefore, PS joints are only used at bottom joint where F_m^{TC} is larger than F_m^0.

Step 4 investigates the unbalanced forces generated by the arch action under different bottom chord member loss scenarios on the bottom joints where PS joints are used. AP analysis is performed on the truss by removing the bottom chord members one at a time. Previous discussions on analysis procedures employed to perform AP analysis in step 2 can also apply for the AP analysis in this step. For each bottom joint BJm where PS joint are used, the unbalanced force following the removal of a bottom chord member BCp can be calculated through

$$F_m^{BCp} = \left| T_m^{BCp} - T_{m+1}^{BCp} \right| \tag{11}$$

Step 5 determines the design sliding resistance for the PS joints. In ideal condition, the design sliding resistance for a bottom joint (R_m) can be determined as the larger of the unbalanced force under design loads F_m^0 and the maximum unbalanced force under arch action F_m^{BC} (maximum F_m^{BCp}). Considering the potential overloading and the possible inaccuracy of the AP analysis results due to model simplification, an amplification factor may be introduced (take a value of 1.1 for example), thus:

$$R_m = 1.1 \times \max\left(F_m^0, F_m^{\mathrm{BC}}\right) \tag{12}$$

For certain bottom joints, sometimes the unbalanced force under arch action may be larger than the unbalanced force under catenary action, indicating that the sliding mechanism under catenary action will not be activated when Eq. 12 is satisfied. In this situation, PS joints are not needed at these bottom joints for the same reason mentioned previously. Alternatively, PS joints can still be still adopted, but in order to examine the effect of releasing the unbalanced forces between the bottom chord members on the proper function of the arch action, detailed numerical investigation that can simulate the sliding of PS joints along the bottom chord as presented above has to be performed.

6. Performance of PS joints under different member-loss scenarios

In this section, three numerically simulated cases are presented to show the performance of PS joints in truss-PSJ subjected respectively to the loss of i) a diagonal member, ii) a top chord member, and iii) a bottom chord member. In order to facilitate a more general application of the PS joints under other member loss scenarios, PS joints in truss-PSJ are re-designed following the method presented above. The modelling approach for the sliding joints, along with the general modelling considerations, follows the validated FE model as described in the previous section.

6.1. Design of PS joints in the new truss-PSJ

Fig. 14 shows the results of the sliding resistance design. The AP analysis in step 2 and step 4 are performed using a nonlinear static analysis procedure with a dynamic increase factor of 1.4. Considering the bilateral symmetric configuration of the truss, there are only two top chord member removal scenarios and three bottom chord member removal scenarios. It is concluded from step 1 to step 3 that PS joints are to be used at BJ2 and BJ3 (the removal of TC3 shall increase the unbalanced force of BJ3). Through step 4 and step 5, the design sliding resistances of BJ2 and BJ3 are determined as R_{BJ2}=R_{BJ3}=1.1×2.55 kN =2.8 kN. All other joints, including all four top joints and bottom joint BJ1 and BJ4, use the standard pinned joint connectors. This new truss model is referred as truss-PSJ-new to distinguish it from the truss model in the experimental program (truss-PSJ).

6.2. Case 1: Removal of DM2

The sliding resistance of BJ2 in truss-PSJ-new is much less than that being used in truss-PSJ, therefore, the study on DM2 removal scenario helps to investigate the effect of different sliding resistances.

The removal of DM2 leads to catenary action along the bottom chord and generates an increased unbalanced force at BJ2. As shown in Fig. 15a, the unbalanced force required to trigger the sliding mechanism of BJ2 is reached at about 0.16 s, and then the unbalanced force of this joint is largely released. The final sliding distance is about 157 mm. It is noted that although the sliding start time is 0.05 s ahead of that in the FE model of truss-PSJ, the sliding distance and the re-balanced deformation shape of the remaining structure are almost identical for these two FE models. Fig. 15b further compares the vertical displacement histories at the mid-span of the top chord. The results match well with only a very small difference after 0.16 s due to the different sliding start times.

Different sliding resistances will tend to result in different sliding start times, but the sliding distance and the associated re-balanced state are determined by the force flow of the remaining structure and thus should not be affected significantly. Therefore, although there can be many possible choices of design sliding resistance, it is reasonable to design the sliding resistance to be just above the minimum sliding resistance demand (Eq. 12), to ensure a timely activation of the sliding mechanism of the PS joints following a triggering event.

6.3. Case 2: Removal of TC1

When initial local failure occurs at a top chord member, the catenary action shall develop along the bottom chord, and the PS joints are expected to play a similar role in maximizing the function of the catenary action as they do under the diagonal member loss scenario. Herein TC1 is chosen as the removed top chord member to examine the performance of the PS joints.

As shown in Fig. 16a, the sliding mechanism of BJ2 is activated at about 0.17 s after TC1 is removed. This is very close to the DM2 removal case because for truss-PJ with non-slidable joints the removal of DM2 and TC1 lead to almost identical deformation shapes (refer to Fig. 13) and thereby similar unbalanced forces of the bottom joints. Fig. 16b shows the re-balanced deformation shape of the remaining structure with a sliding distance of BJ2 being about 159 mm, which is also very close to the DM2 removal case.

6.4. Case 3: Removal of BC3

Among all bottom chord members, the removal of BC3 leads to the largest unbalanced forces at BJ2 and BJ3, thus this scenario is investigated.

When BC3 suddenly fails, arch action is developed to provide the bridge-over capacity for the remaining structure. Fig. 17a shows the unbalanced forces at BJ2 and BJ3. It is noted that the unbalanced forces have always been below the design sliding resistance of the PS joints, thus the sliding mechanism of both joints is not activated. The remaining structure regains a balanced state easily with its original position maintained, as shown in Fig. 17b.

7. Conclusions

This paper presents a study on a new type of truss joint, called Pinned-Slidable or PS joint, for enhancing the progressive collapse resistance of planar trusses. A PS joint stays fixed on the bottom chord without sliding under the design loads, but can slide along the bottom chord to help distribute the unbalanced tensile forces that the catenary action generates in different bottom chord members in a member removal scenario. The working mechanism of the PS joint has been explained in detail, and a full design approach has also been provided for implementation of this new type of truss joint in practice. An experimental study has been carried out on a warren truss with the PS joints as the bottom joints (truss-PSJ) under a sudden removal of a diagonal members, and the response is compared with that of its conventional counterpart with non-slidable joints (truss-PJ). Finite element analyses have also been conducted to further examine the performance of PS joints under different progressive collapse scenarios. The following main conclusions may be drawn:

(1) The sliding resistance of the PS joint can be controlled through the pressure applied by the preloaded bolts and the size of the locking rod, which can be designed according to the design schemes proposed in this paper. Two design schemes for the PS joints may be adopted, namely, a) the “strong bolts, weak rod” scheme, in which the design sliding resistance is fully achieved by the static friction generated by the preloaded bolts, and b) the “weak bolts, strong rod” scheme, in which the design sliding resistance is achieved by both the kinetic friction generated by the preloaded bolts and the shear resistance of a locking rod.

(2) Results from the experiments demonstrate that much larger tensile forces develop in the mid-span area of the bottom chord members than in the neighboring bottom chord members after the removal of a diagonal member, leading to the actual sliding of a PS joint. The sliding of the PS joint not only releases the excessive unbalanced forces between neighboring members and thus enables a fuller development of the catenary action, but also facilitates the adaptation of the remaining structure towards a new balanced state with a near-optimal deformation shape.

(3) Finite element analyses demonstrate that the proposed design procedure for the sliding resistance of the PJ joints is effective in that sliding of the PS joints can be timely realized when necessary, and thereby improves the overall progressive collapse resistance of the truss structures.

The experimental and numerical studies in this paper have been focused on the PS joints with a “strong bolts, weak rod” design. Although the same principle applies, further investigations into the actual effectiveness of PS joints with a “weak bolts, strong rod” design is useful and this extended work is currently underway. Meanwhile, the concept of the PS joints represents an attempt to develop an adaptive truss system that would lead to maximization of the resistance of the structure against accidental exposures. To this end, further investigations are still needed to improve and optimize the design of the PS joint and explore possible use of other types of structural connections with adaptive functions.

Acknowledgement

The work presented in this paper was funded by the National Natural Science Foundation of China (No. 51678432). The authors would like to thank Xiao-hua Tong (College of Surveying and Geoinformatics in Tongji University) for their assistance in 3D displacement measurement by means of videogrammetric technique. The help provided by Tian-lang Peng (Earthquake Engineering Building in Tongji University) during the experiment program is also appreciated.

References

[1] Smith EA, Epstein HI. Hartford coliseum roof collapse: Structural collapse sequence and lessons learned. Civil Eng 1980; 50(4):59–62.

[2] National Transportation Safety Board (NTSB). Highway accident report, collapse of I-35W highway bridge, Minneapolis, Minnesota August 1, 2007. NTSB/HAR-08/03PB, Washington, DC; 2008.

[3] Ma X, Han B. Analysis and Mitigation of Progressive Collapse for Steel Truss Girders. In: Int Conf Mech Autom Control Eng, MACE -

Proc. Piscataway, NJ: IEEE Computer Society; 2011, p.1931-4.

[4] Jiang X, Chen Y. Progressive collapse analysis and safety assessment method for steel truss roof. J Perform Constr Facil 2012; 26(3):230-40.

[5] Yan S, Zhao X, Lu Y. Collapse-resisting mechanisms of planar trusses following sudden member loss. J Struct Eng 2017; 143(9):04017114.

[6] Zhao X, Yan S, Chen Y, Xu Z, Lu Y. Experimental study on progressive collapse-resistant behavior of planar trusses. Eng Struct 2017; 135:104-16.

[7] Chen Y, Zhao X, Wang L, Yan S. Progressive collapse of large span truss-beam structures induced by initial member break. In: Saf, Robust Cond Assess Struct. Zurich, Switzerland: IABSE; 2015, p.112-9.

[8] Miyachi K, Nakamura S, Manda A. Progressive collapse analysis of steel truss bridges and evaluation of ductility. J Constr Steel Res 2012; 78:192–200.

[9] URS Corporation. Fatigue evaluation and redundancy analysis, Bridge No. 9340, I-35W over Mississippi River. Draft Rep. Prepared for Minnesota Dept. of Transportation, Minneapolis; 2006.

[10] Goto Y, Kawanishi N, Honda I. Dynamic stress amplification caused by sudden failure of tension members in steel truss bridges. J Struct Eng 2011; 137(8):850-61.

[11] Khuyen HT, Iwasaki E. An approximate method of dynamic amplification factor for alternate load path in redundancy and progressive collapse linear static analysis for steel truss bridges. Case Stud Struct Eng 2016; 6:53-62.

[12] American Institute of Steel Construction (AISC). Specification for Structural Steel Buildings. AISC360-10. Chicago: American Institute of Steel Construction; 2010.

[13] Oberg E, Jones FD, Horton HL, Ryffel HH. Machinery's Handbook, 29th Edition. New York: Industrial Press; 2012.

[14] Zhao X, Yan S, Chen Y. Comparison of progressive collapse resistance of single-layer latticed domes under different loadings. J Constr Steel Res 2017;129:204-14.

[15] Kwan JSH, Chan SL, Cheuk JCY, Koo RCH. A case study on an open hillside landslide impacting on a flexible rockfall barrier at Jordan

Valley, Hong Kong. Landslides 2014; 11(6): 1037-1050.

[16] Department of Defense (DOD). Design of buildings to resist progressive collapse. Unified Facilities Criteria (UFC) 4-023-03. Washington, DC: Department of Defense; 2009.

Figure

(a)

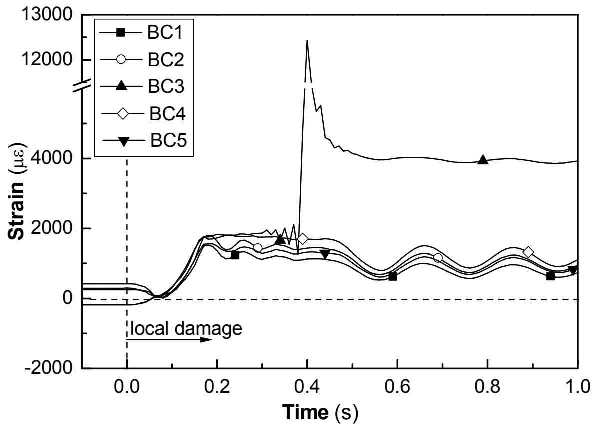

(b)

Fig. 1. Catenary action developed under a diagonal member loss scenario in the truss-PJ test in [6]. (a) Re-balanced state; (b) axial strains in bottom chord members.

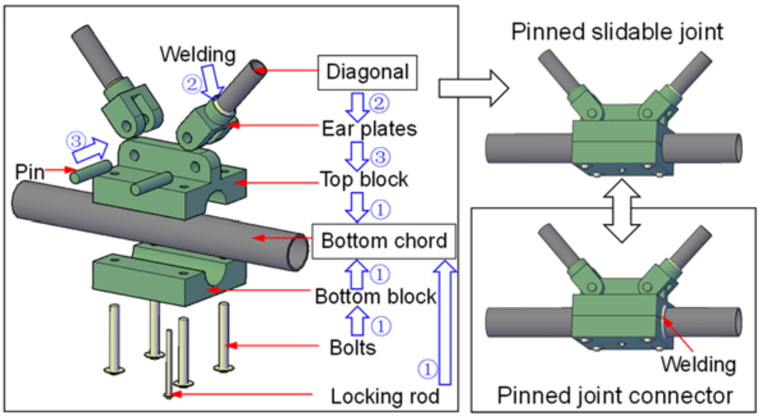

Fig. 2. Pinned slidable joint.

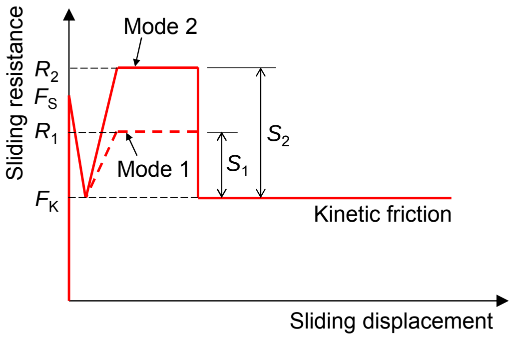

Fig. 3. Sliding resistance of a PS joint with two possible modes.

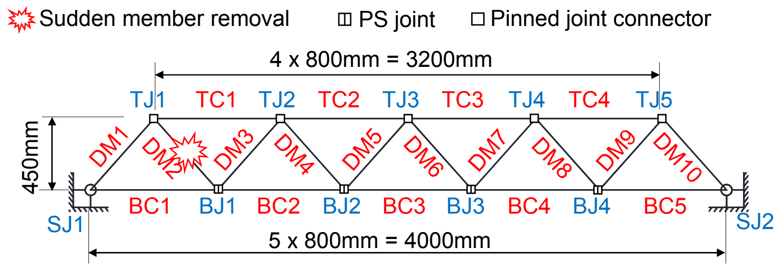

Fig. 4. Overview of truss-PSJ and designation of members and joints.

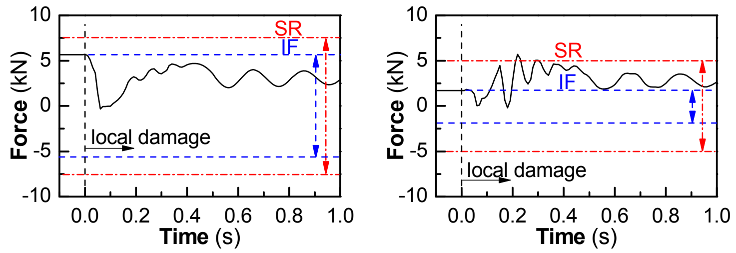

(a) (b)

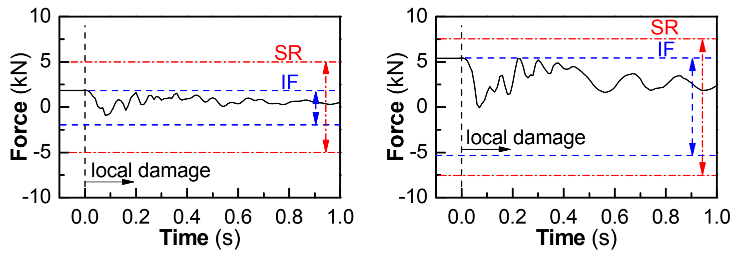

(c) (d)

Fig. 5. Unbalanced force histories of the bottom joints in truss-PJ, and the immobilizing force (IF) and the sliding resistances (SR) of the PS joints in truss-PSJ. (a) BJ1; (b) BJ2; (c) BJ3; (d) BJ4.

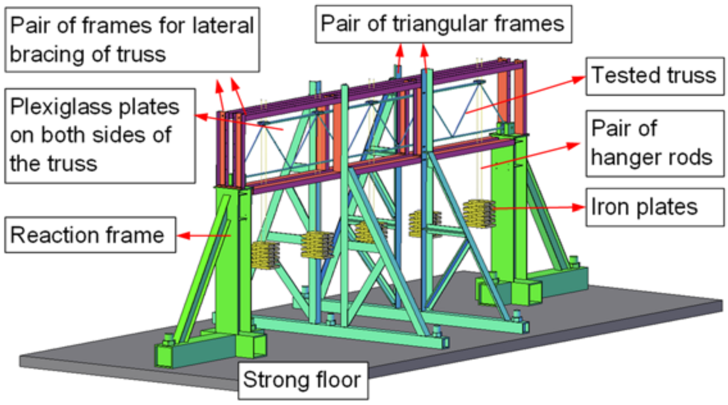

Fig. 6. Test setup

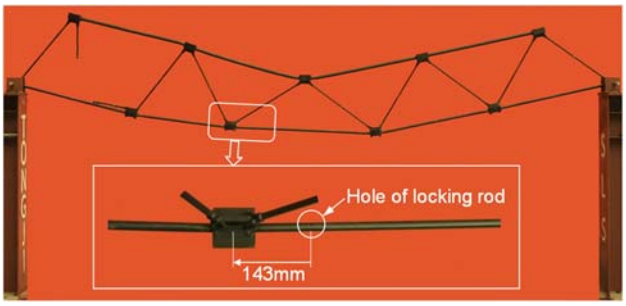

(a)

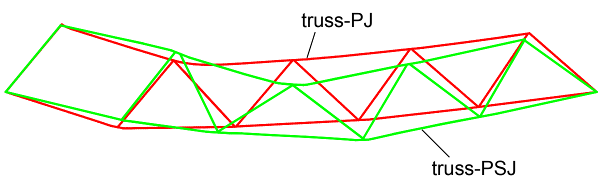

(b)

Fig. 7. Re-balanced state of truss-PSJ following the removal of DM2. (a) BJ2 slid along the bottom chord for 143mm; (b) comparison between truss-PSJ and truss-PJ.

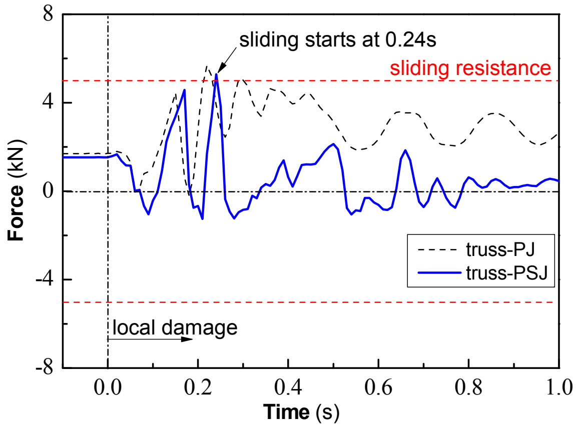

(a)

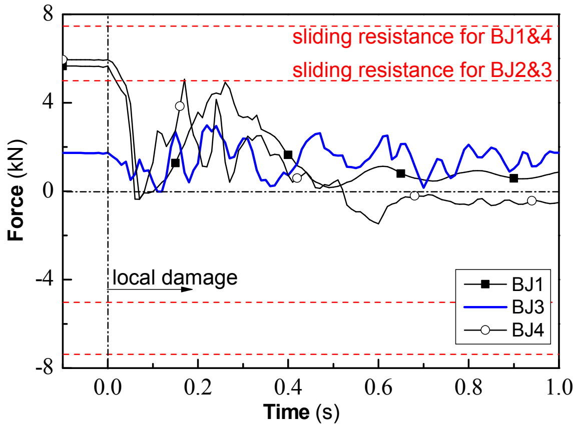

(b)

Fig. 8. Unbalanced force of bottom joints. (a) BJ2; (b) BJ1, BJ3 and BJ4.

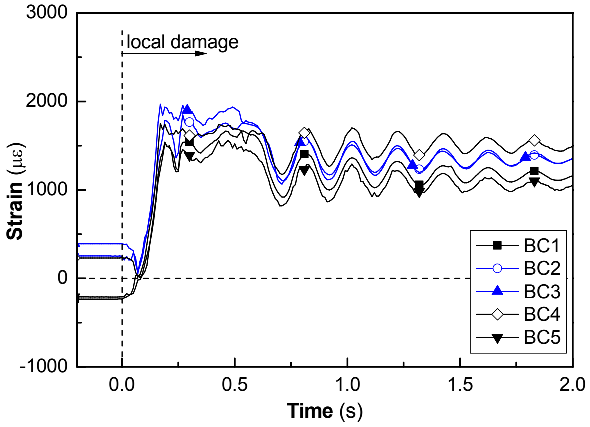

(a)

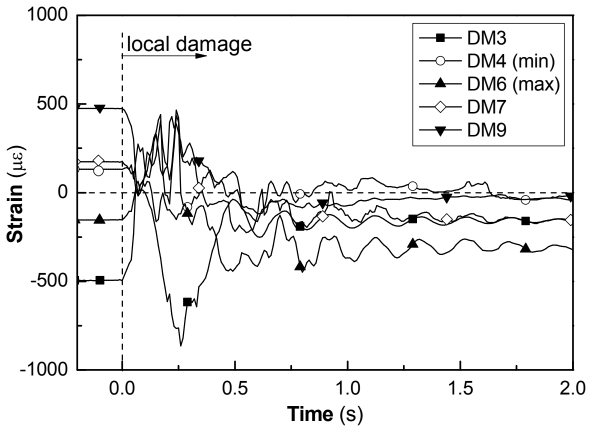

(b)

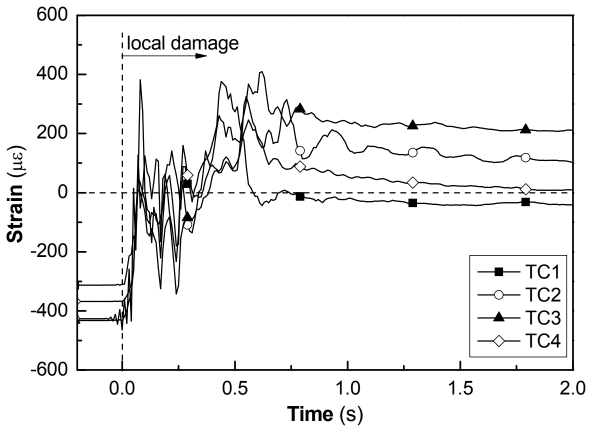

(c)

Fig. 9. Axial strain in members of truss-PSJ. (a) Bottom chord members; (b) diagonal members; (c) top chord members.

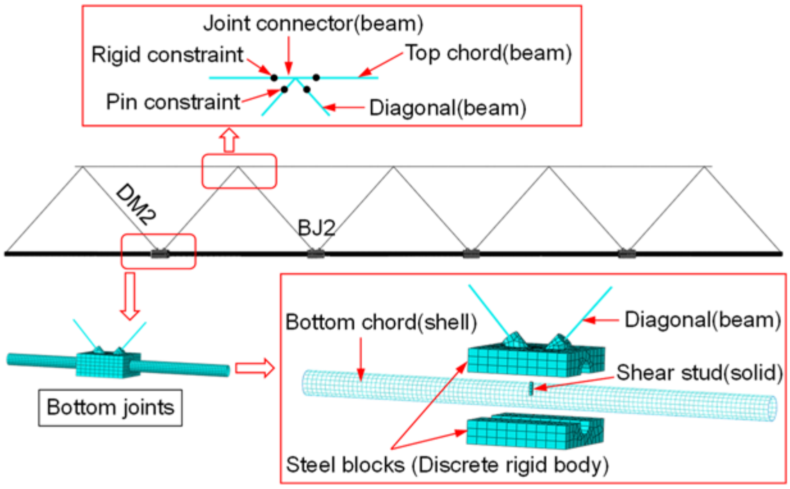

Fig. 10. FE model of truss-PSJ

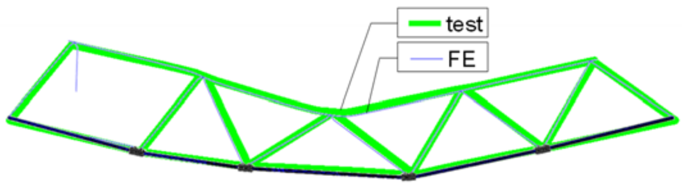

(a)

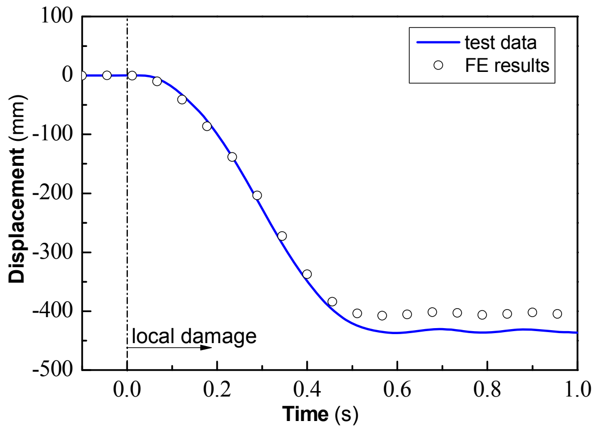

(b)

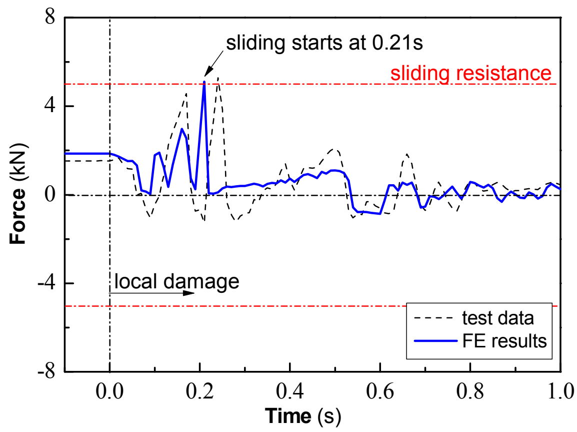

(c)

Fig. 11. Comparison of test and FE results of truss-PSJ. (a) Balanced configuration; (b) vertical displacement of TC3; (c) unbalanced force of BJ2.

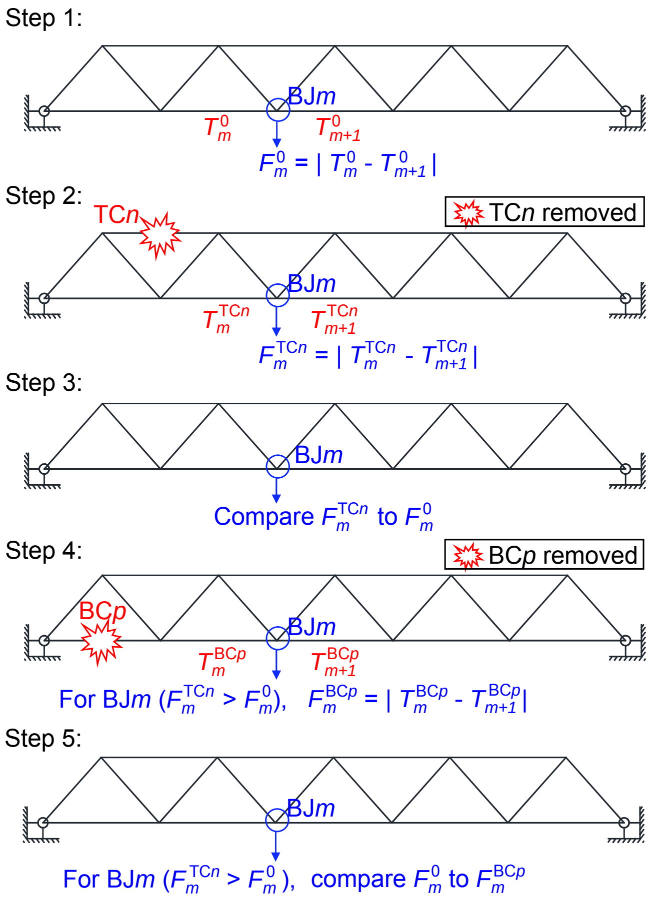

Fig. 12. Method for sliding resistance design of PS joints.

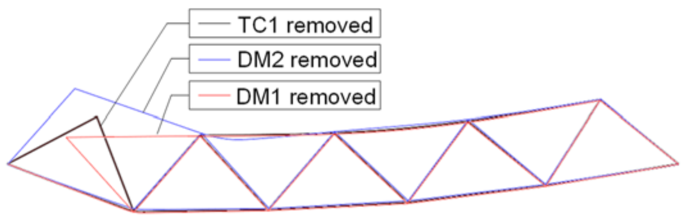

Fig. 13. Re-balanced deformation shapes of truss-PJ subjected to removal of TC1, DM1 and DM2.

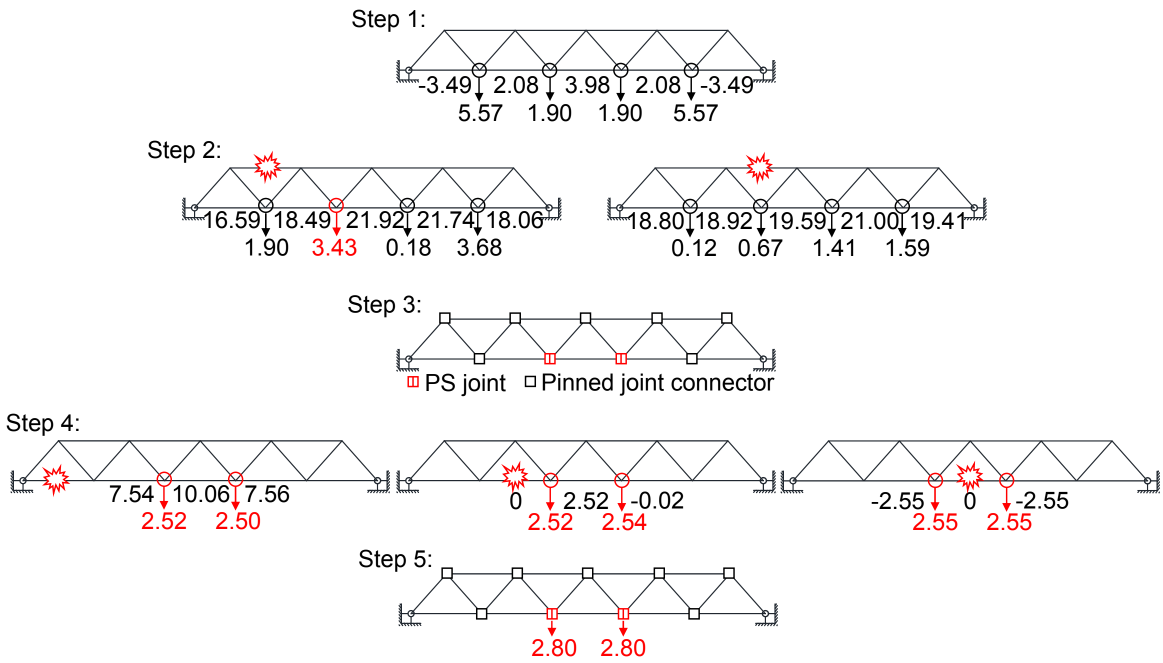

Fig. 14. Design of PS joints for truss-PSJ-new. (Unit: kN)

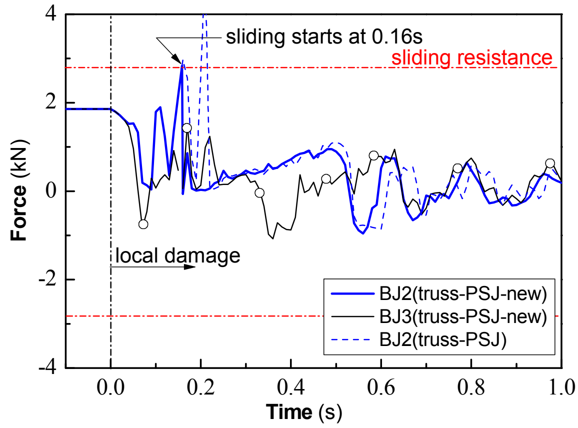

(a)

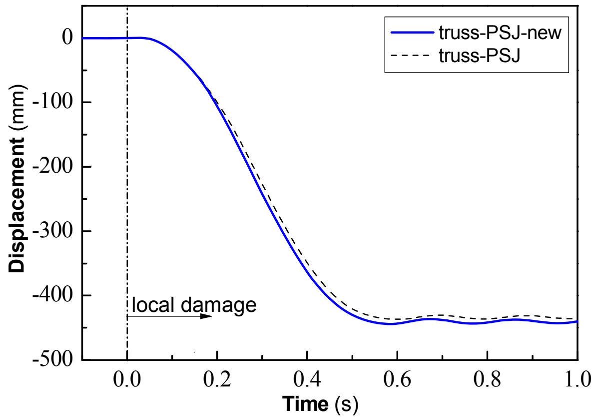

(b)

Fig. 15. Results of truss-PSJ-new following removal of DM2 and their comparison against truss-PSJ. (a) Unbalanced force of BJ2 and BJ3; (b) vertical displacement of TJ3.

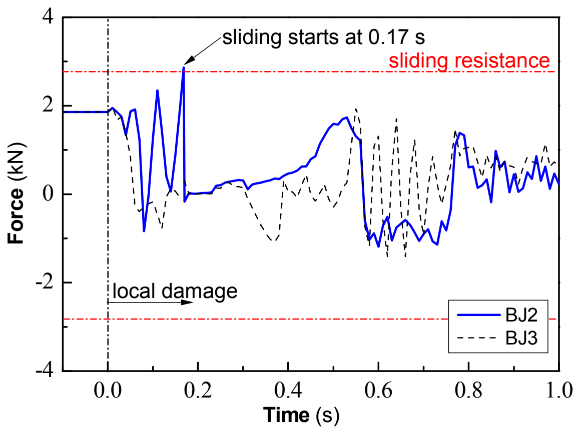

(a)

(b)

Fig. 16. Results of truss-PSJ-new following removal of TC1. (a) Unbalanced force of BJ2 and BJ3; (b) Re-balanced deformation shape.

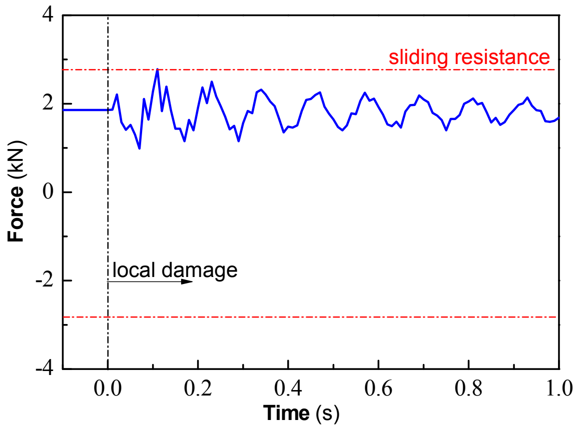

(a)

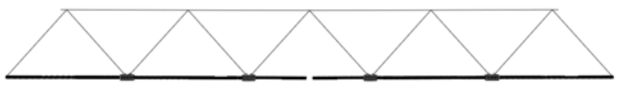

(b)

Fig. 17. Results of truss-PSJ-new following removal of BC3. (a) Unbalanced force of BJ2 and BJ3; (b) Re-balanced deformation shape.

Tables

Table 1. Cross-sections and mechanical properties of members

	Cross-section	Yield strength f_y (MPa)	Ultimate strength f_u (MPa)	Fracture strain ε_u[a]
TC	$\phi 25\times1.5$	300	409	0.26
BC	$\phi 20\times1$	305	418	0.26
DM	$\phi 14\times1$	278	415	0.35

[a] Fracture strain is based on proportional coupon gauge length of $5.65\sqrt{S_0}$, where S_0= original cross-section area of coupons.